

Barotropic Process Contributing to the Formation and Growth of Tropical Cyclone Nargis

MAO Jiangyu* (毛江玉) and WU Guoxiong (吴国雄)

State Key Laboratory of Numerical Modeling for Atmospheric Sciences and

Geophysical Fluid Dynamics, Institute of Atmospheric Physics,

Chinese Academy of Sciences, Beijing 100029

(Received 20 March 2010; revised 18 June 2010)

ABSTRACT

This study reveals the barotropic dynamics associated with the formation and growth of tropical cyclone Nargis in 2008, during its formation stage. Strong equatorial westerlies occurred over the southern Bay of Bengal in association with the arrival of an intraseasonal westerly event during the period 22–24 April 2008. The westerlies, together with strong tropical–subtropical easterlies, constituted a large-scale horizontal shear flow, creating cyclonic vorticity and thereby promoting the incipient disturbance that eventually evolved into Nargis. This basic zonal flow in the lower troposphere was barotropically unstable, with the amplified disturbance gaining more kinetic energy from the easterly jet than from the westerly jet during 25–26 April. This finding suggests that more attention should be paid to the unstable easterly jet when monitoring and predicting the development of tropical cyclones. Energetics analyses reveal that barotropic energy conversion by the meridional gradient of the basic zonal flow was indeed an important energy source for the growth of Nargis.

Key words: tropical cyclone, tropical–subtropical easterlies, barotropic instability

Citation: Mao, J. Y., and G. X. Wu, 2011: Barotropic process contributing to the formation and growth of tropical cyclone Nargis. *Adv. Atmos. Sci.*, **28**(3), 483–491, doi: 10.1007/s00376-010-9190-4.

1. Introduction

One of the favorable environmental factors for tropical cyclone (TC) formation is sea surface temperature (SST) above 26°C (Gray, 1968, 1975). The North Indian Ocean (NIO) is climatologically the warmest area of tropical ocean during April and May, prior to the onset of the south Asian summer monsoon (Shenoi et al., 1999); thus, TCs in the NIO tend to form between April and December, with a principal peak in occurrence during October–December and a secondary peak during April–June (Holland, 1993; Kikuchi et al., 2009). In 2008, SST in the NIO had reached 29°C–30°C by 17 April (McPhaden et al., 2009). Subsequently, the first TC (named “Nargis” by the Indian Meteorological Department) developed in the Bay of Bengal (BOB) on 27 April. The Joint Typhoon Warning Center (JTWC) classified this storm as Tropical Cyclone 01B. The cyclone rapidly intensified to be-

come a very severe storm by 0600 UTC on 28 April and eventually made landfall in the Ayeyarwady Division of Myanmar at around 1200 UTC on 2 May, causing widespread destruction of buildings and tens of thousands of fatalities. Aside from the favorable oceanic conditions during middle–late April 2008 (McPhaden et al., 2009), there remains uncertainty regarding which dynamical processes were responsible for the formation and rapid growth of such a strong cyclone. The aim of the present study is to identify the relevant processes in this regard.

As demonstrated by Gray (1975), under favorable thermodynamic conditions, the development of a TC depends largely on the dynamic conditions of large-scale atmospheric circulation. Harr and Elsberry (1995) and Chen and Huang (2008) suggested that the location of the monsoon trough is the primary control on the distribution of TC activity in the western North Pacific. Thus, most TCs form within or immediately

*Corresponding author: MAO Jiangyu, m jy@lasg.iap.ac.cn

poleward of the ITCZ and monsoon trough (e.g. Gray, 1975; Zehr, 1992).

In the Indian Ocean, the monsoon trough moves slowly northward from February to April and then swings quickly across the BOB in May. The zone of TC development moves northward with the monsoon trough (Gray, 1968). During the transition season, the monsoon trough and ITCZ occur on both sides of the equator near 5°N and 5°S ; thus, twin cyclones sometimes occur in the southern BOB (Ferreira and Schubert, 1996). In fact, Nargis originated from one cyclone of a pair that occurred around 23 April 2008 (Kikuchi et al., 2009). The cyclone pair was observed on both sides of the equator in the Indian Ocean at 1200 UTC on 23 April, with a strong equatorial westerly flow between them.

Kikuchi et al. (2009) related this equatorial westerly flow to the arrival of an intraseasonal westerly event into the southern BOB during the period 22–24 April 2008. They also suggested that Nargis was initiated by such an intraseasonal westerly event. Actually, Liebmann et al. (1994) showed that TCs in the Indian and western Pacific oceans preferentially occur during the convective phase of the Madden–Julian oscillation (MJO; Madden and Julian, 1994). The MJO is a planetary-scale eastward-propagating wave-like disturbance of the tropical atmosphere with coherent fluctuations in winds and convection (e.g. Wheeler and Hendon, 2004; Zhou and Chan, 2005), which may modulate tropical cyclogenesis (e.g. Mao and Wu, 2010). Ferreira and Schubert (1996) used a nonlinear shallow-water model to examine dynamical aspects of the formation of twin TCs by MJO convection. They revealed that MJO convection can produce twin tropical disturbances in the eastern Indian Ocean, with the necessary condition for barotropic instability being satisfied by the equatorial westerly flow that lies between the two cyclones (Eliassen, 1983), which suggests that barotropic instability may play a role in TC formation.

In fact, many researchers have noted the importance of barotropic instability of large-scale zonal flow during the tropical cyclogenesis process (e.g. Krishnamurti et al., 1981; Mishra et al., 1985; Guinn and Schubert, 1993; Ferreira and Schubert, 1997). Nitta and Masuda (1981) analyzed a monsoon depression that developed over the BOB in the summer of 1979. During the formative stage of the depression, its horizontal trough axis was found to be inclined from southwest to northeast, with a barotropically unstable westerly jet located mainly south of the trough axis, which favored the depression gaining its kinetic energy from the zonal mean flow due to northward transport of the westerly momentum. Subrahmanyam

et al. (1981) used a two-layer model to examine the mechanisms for the formation and intensification of the same depression as studied by Nitta and Masuda (1981). Their numerical solutions showed that the wavelength of the divergent barotropic preferred wave was in good agreement with the observed wavelength, with poleward momentum transports predominating over equatorward transports. Based on a monsoon onset vortex formed in the Arabian Sea during June 1979, George and Mishra (1993) investigated the relative roles of barotropic and baroclinic processes in its initial growth. They found that the barotropic conversion from zonal kinetic energy to eddy kinetic energy dominated over the baroclinic conversion from eddy available energy to eddy kinetic energy. These findings indicate that barotropic instability does indeed play a positive role during the initial formation and growth of TCs.

The primary feature associated with the initial formation of TCs in the above case studies was that a barotropically unstable westerly jet as the basic zonal flow located south of the trough axis, and it supplied kinetic energy for TC growth. As compared with other TCs in previous studies (e.g. Nitta and Masuda, 1981; George and Mishra, 1993), however, Nargis in 2008 exhibited a remarkable difference in terms of its large-scale circulation structure during the formative stage. The most outstanding feature of Nargis was that besides the unstable equatorial westerly jet, there was a strong easterly jet between roughly 10° and 15°N (as shown in Fig. 1). Therefore, the role of such a tropical–subtropical easterly flow in the rapid growth of Nargis needs to be understood.

Although baroclinic instability associated with the diabatic process may also be involved in TC development (e.g. George and Mishra, 1993), the role which this process plays takes place mainly in the mature stage of a TC. As was demonstrated by Maloney and Hartmann (2001), latent heat release is important to developing and mature TCs, and mature TCs are characterized by strong vertical shears away from their center.

Liebmann et al. (1994) suggested that dynamical conditions of large-scale circulations appear to have greater impacts on whether a depression initially develops than whether an existing depression intensifies further. Since barotropic instability plays a dominant role during the initial growth of TCs, it is conceivable that the barotropic process arising from strong horizontal shear of tropical–subtropical easterly flow in combination with the equatorial westerly flow might represent an important mechanism for the rapid growth of Nargis. Therefore, the objective of this study is to reveal the barotropically dynamical process

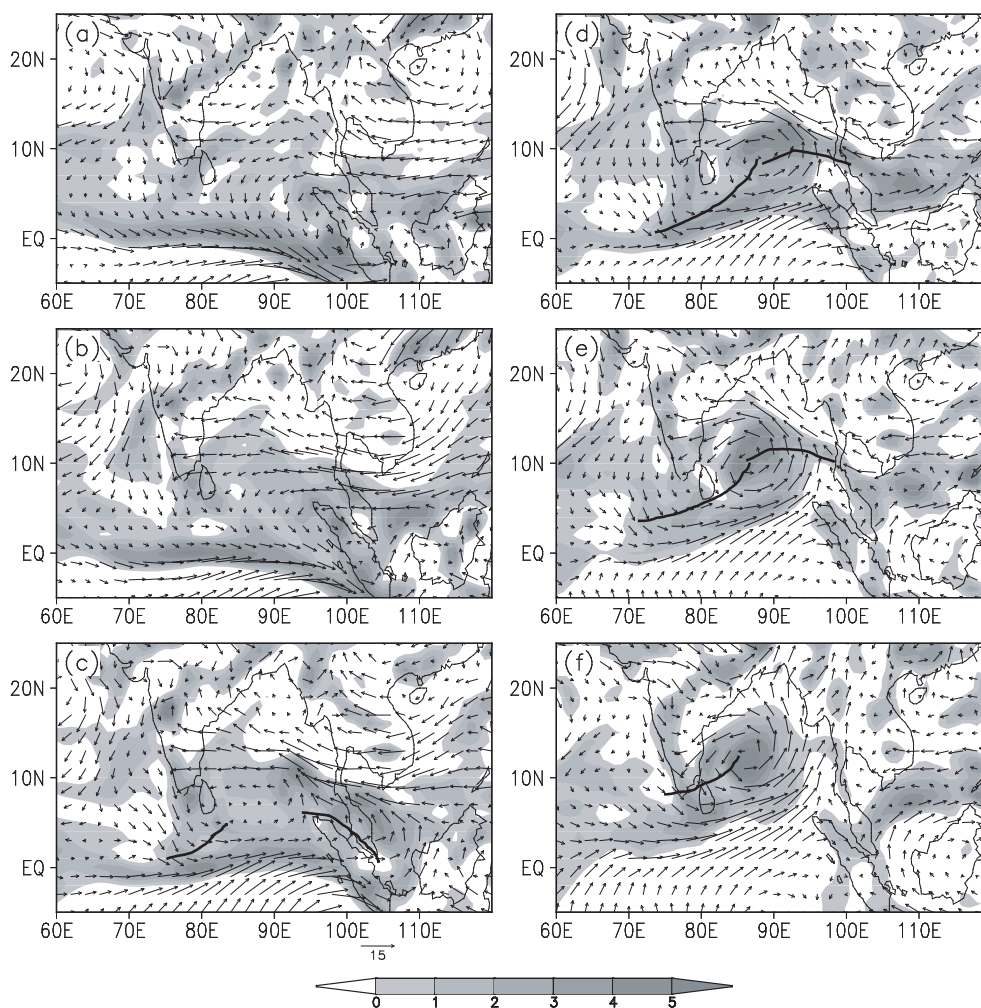


Fig. 1. Evolution of daily mean low-level winds (vectors, m s^{-1}) and relative vorticity (shaded, 10^{-5} s^{-1}) at 850 hPa from (a) to (f) for the period 22–27 April 2008, respectively. The thick solid line indicates the trough axis.

of the unstable lower tropospheric zonal flow that contributed to the formation and growth of Nargis during its formation stage.

To do this, we employed the National Centers for Environmental Prediction (NCEP) Final (FNL) analysis dataset because of its high horizontal resolution ($1^\circ \times 1^\circ$ grid). These products are actually derived from the Global Forecast System (GFS), which is operationally run four times a day; thus, they are available every 6 hours at 26 pressure levels from 1000 to 10 hPa.

2. Evolution of low-level circulation and development of Nargis

Figure 1 shows the evolution of the daily mean low-level winds and relative vorticity at 850 hPa before and during the development of Nargis. On 22 April

(Fig. 1a), an elongated strip with maximum relative vorticity greater than $3 \times 10^{-5} \text{ s}^{-1}$ occurred along the equator west of Sumatra, probably due mainly to the horizontal shear associated with equatorial westerlies. Note that a semi-closed large-scale cyclonic circulation appeared around the eastern end of the strong equatorial westerly flow, with the center of maximum vorticity located near Sumatra. On 21 April, there were two off-equatorial vortices in the southern Indian Ocean along with a cloud cluster in the NIO (Kikuchi et al., 2009), although no vortex was observed to correspond to the cluster. Therefore, the cyclonic circulation (Fig. 1a) could have arisen via the response of the tropical atmosphere to convective heating (Gill, 1980; Zehr, 1992).

Subsequently, a cyclonic center appeared over the northwest tip of Sumatra Island on 23 April, with rapidly increasing positive vorticity (Fig. 1b). This

cyclonic center could be interpreted as the incipient disturbance that eventually evolved into Nargis, as shown by Kikuchi et al. (2009), who suggested that Nargis was initiated by an intraseasonal westerly event associated with the arrival of the MJO at the western Maritime Continent. Of note is the fact that strong easterlies prevailed from the western North Pacific to the Indian subcontinent north of 5°N , with the easterly jet located at around 10°N (Figs. 1a and 1b). These strong tropical–subtropical easterlies and the equatorial westerlies made up of a large-scale parallel shear flow, created cyclonic vorticity over the southern BOB; consequently, the increasing low-level vorticity may have been dominated by shear vorticity. As discussed below, this basic shear flow was barotropically unstable, thereby favoring growth of the incipient disturbance via barotropic eddy–mean flow interactions.

By 24 April (Fig. 1c), a newly developed positive vorticity center (around 12.5°N , 92.5°E) with a maximum greater than $3 \times 10^{-5} \text{ s}^{-1}$ had developed on the northern side of a huge, closed large-scale cyclonic circulation over the southern half of the BOB. Note that the easterly jet had moved slightly northward compared with its position on the previous day. Associated with this larger cyclone was a weak horizontal trough south of Sri Lanka and north of the equator, which comprised strong equatorial westerlies and northwesterlies to the north. The axis of the trough was oriented NE–SW and the maximum westerly flow was located south of the trough axis. This trough enabled the poleward transport of westerly momentum, with transport occurring down the gradient of basic zonal flow (Nitta and Masuda, 1981; Subrahmanyam et al., 1981), leading to conversion of the basic state kinetic energy into disturbance kinetic energy. A huge cyclonic circulation developed over the NIO, with another trough, oriented NW–SE, located along the northeast coast of Sumatra. Subsequently, the cyclonic circulation underwent a marked contraction, such that a TC-scale depression formed over the central BOB, with equatorial westerlies extending northward (Fig. 1d).

At 1200 UTC on 25 April, the JTWC issued a TC warning regarding the tropical depression that had formed at (10.5°N , 90.3°E). The axis of the NE–SW-oriented trough was strongly elongated through the cyclone center, enhancing the growth rate of the depression because the depression kinetic energy was supplied from both easterly and westerly currents (Nitta and Yanai, 1969; Subrahmanyam et al., 1981). Consequently, the system rapidly intensified into a deep depression during 26 April (Fig. 1e), and further developed into a storm on 27 April (Fig. 1f), with relative vorticity in the storm center exceeding $5 \times 10^{-5} \text{ s}^{-1}$. The depression migrated northwestward as it rapidly

strengthened.

Compared with previous days, the easterlies over the Indian subcontinent and South China Sea showed a marked weakening; the JTWC best-track data also showed that rapid intensification occurred mainly during these two days (26–27 April). Nitta and Yanai (1969) showed that for a moderate horizontal shear of zonal currents, the growth rate of amplified disturbances in the easterlies is larger than that in the westerlies; thus, the tropical–subtropical easterlies may have made a greater contribution to the growth of Nargis during this developing stage than did the equatorial westerlies.

As suggested by Krishnamurti et al. (1981), the barotropic instability of a zonal flow with horizontal shear can be examined based on the meridional gradient of absolute vorticity. The zonally-averaged meridional gradient of absolute vorticity is given by

$$[M] = -\frac{\partial^2}{\partial y^2}[u] + \beta, \quad (1)$$

where M represents the meridional gradient of absolute vorticity, u is the zonal wind, β denotes the meridional gradient of the Coriolis parameter, and square brackets indicate the zonal average. Considering its spatial scale, the disturbance is separated from the zonal mean flow averaged between 70°E and 110°E . This larger longitudinal range is used in calculating the zonal average to ensure complete separation of the mean flow and the disturbance. The choice of such a longitudinal range may also avoid the edge effect of unreasonable eddy energy convergence from the selected boundaries in quantitatively diagnosing barotropic energy conversions (as discussed in section 3).

On 25 April (Fig. 2a), a zero line of zonal flow existed near 7.5°N in the middle and lower troposphere (from the surface to 400 hPa), with a large easterly jet to the north. The maximum westerly was present mainly in the lower troposphere south of 2.5°N . Correspondingly, the negative meridional gradient of absolute vorticity occurred between 9°N and 14°N , with positive gradients to the south and north; i.e. the meridional gradient of absolute vorticity possessed both signs in the meridional plane on an isobaric surface in the middle and lower troposphere, indicating that the zonal flow over the NIO satisfied the necessary conditions for barotropic instability of internal jets (e.g. Kuo, 1949; Eliassen, 1983).

Theoretically, an unstable zonal flow is only able to supply the energy needed for the growth of disturbances in the case that the mean zonal flow is positively correlated with the meridional gradient of absolute vorticity (Eliassen, 1983). Note that in the

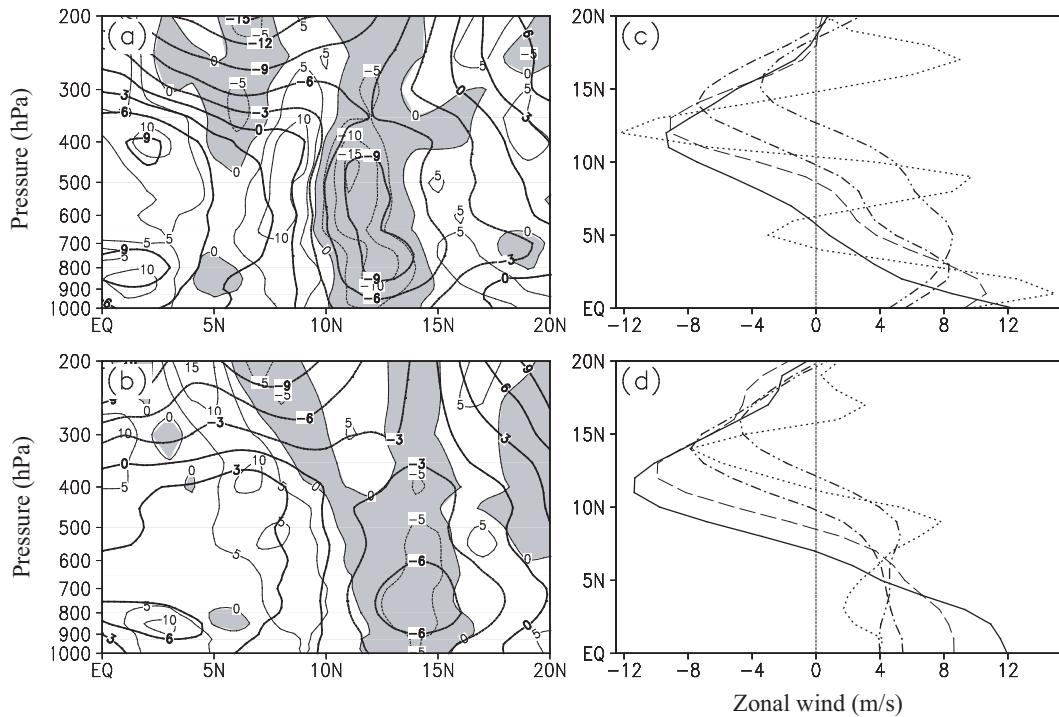


Fig. 2. (a) Latitude–pressure cross section (70° – 110° E) of daily mean zonal wind (thick contours; isotach interval, 3 m s^{-1}) and meridional gradient of absolute vorticity (thin contours; isoline interval, $5 \times 10^{-11} \text{ s}^{-1} \text{ m}^{-1}$; negative values are shaded) for 25 April 2008. (b) As in (a) except for 26 April. (c) Meridional profiles of daily mean 850-hPa zonal winds (m s^{-1}) for 24 April (solid curve), 25 April (long-dashed curve), 26 April (dot-dashed curve), 27 April (dot-dot-dashed curve), and meridional gradient of absolute vorticity (dotted curve) at 850 hPa for 25 April. (d) As in (c) except for the 700-hPa level and the meridional gradient on 26 April.

present case, the negative gradient coincided with strong easterlies at around 7.5° – 15° N, while the positive gradient corresponded to strong westerlies south of 7.5° N, suggesting a positive correlation between them. Therefore, the basic zonal flow was indeed dynamically unstable, which favored the growth of Nargis via barotropic energy conversion. Compared with 25 April, the unstable basic flow on 26 April extended farther northward (Fig. 2b), and the intensity of the easterly jet weakened to 6 m s^{-1} , with the center of the jet dropping to around 750 hPa.

Although upper tropospheric divergence is important for TC formation in association with a compensating lower-tropospheric convergence, the results of observational studies (e.g., Gray, 1968) indicate that low-level convergence is frictionally forced and that outflow in the upper troposphere is largely determined by processes in the subcloud boundary layer. Thus, in the lower troposphere, dynamical processes that act to increase cyclonic vorticity and moisture convergence are a crucial aspect of TC development.

To further demonstrate such barotropic processes, Fig. 2 shows meridional profiles of daily mean zonal

winds at 850 and 700 hPa. For each day during the period 24–27 April, the 850-hPa zonal wind had a maximum (westerly jet) around the equator and a minimum (tropical–subtropical easterly jet) between 7.5° N and 15° N (Fig. 2c). The meridional gradient of absolute vorticity on 25 April changed its sign at least twice between the equator and 20° N, and its minimum (maximum) coincided with the minimum (maximum) of the mean zonal wind, thereby indicating that the 850-hPa zonal wind satisfied the two necessary conditions for barotropic instability (as shown in Fig. 2a). In fact, similar situations occurred on the other three days of interest. Note that absolute values of wind velocity extreme decreased day-by-day from 24 to 27 April, indicating that Nargis gained its kinetic energy from the mean zonal flow. At 700 hPa (Fig. 2d), such barotropic energy conversion was more pronounced than that at 850 hPa, especially for the day-by-day decrease in maximum easterly velocity with increasing latitude. We also observed a pronounced daily decrease in the maximum velocity of the equatorial westerly. These findings further suggest that the unstable zonal flow at low levels contributed to the rapid

growth of Nargis.

3. Barotropic energy conversion

Because the mean kinetic energy of the unstable zonal flow was a source of energy for the growth of Nargis, it is necessary to examine the relative importance of this barotropic energy conversion. Norquist et al. (1977) and Ross (1991) utilized the energy equations derived by Lorenz (1955) to investigate the energetics of African wave disturbances. Recently, Ross and Krishnamurti (2008) applied this approach in assessing the importance of barotropic energy conversion at 700 hPa for African easterly waves that developed into depressions and storms. As shown by Ross and Krishnamurti (2008), the kinetic energy tendency equation for an eddy, in pressure coordinates and linearized about a basic state ($[u]$, $[v]$), can be written as

$$\frac{\partial}{\partial t} K' \propto -u'v' \frac{\partial [u]}{\partial y} - v'^2 \frac{\partial [v]}{\partial y} - u'\omega' \frac{\partial [u]}{\partial p} - v'\omega' \frac{\partial [v]}{\partial p}, \quad (2)$$

where u and v are the zonal and meridional components of the horizontal winds, respectively; and ω is vertical velocity. The square brackets indicate the zonal mean of the variable for a given time, thus the zonally-averaged variable over a given longitudinal range is used to represent the basic flow. The prime denotes the departure of the variable at a point from the zonal mean, and K' is the eddy kinetic energy represented by $K' = (u'^2 + v'^2)/2$. Note that other terms, such as the conversion of eddy available potential energy to eddy kinetic energy, boundary energy fluxes, and the dissipation of eddy kinetic energy by friction, are not included in Eq. (2) because it is the barotropic energy conversion that is of interest here.

As stated above, the disturbance should be properly separated from the zonal mean flow because a narrow longitudinal extent for the zonal mean would lead to unreasonable eddy energy fluxes from the given boundaries. Thus, the zonal mean is calculated over the longitudinal range from 70°E to 110°E, as in Fig. 2. Figure 3 shows the daily-mean eddy kinetic-energy tendency and related barotropic conversion terms for 25 and 26 April, as on these days the depression intensified more rapidly and a significant NE–SW trough was located over the southern BOB (Figs. 1d and 1e). The increase in eddy kinetic energy recorded on 25 April occurred over the western and central BOB, with a generation rate greater than $1.5 \times 10^{-4} \text{ m}^2 \text{ s}^{-3}$, mainly within the longitudinal band around 90°E (Fig. 3a).

The first term of the rhs of Eq. (2) was the domi-

nant term (Fig. 3b), being at least an order of magnitude greater than the second term (Fig. 3c) and the other terms. There were two areas (i.e. south and north of 10°N) in which the amount of eddy kinetic energy generated exceeded $1.5 \times 10^{-4} \text{ m}^2 \text{ s}^{-3}$ (Fig. 3b). A comparison with Fig. 3a reveals that these areas coincided with the region of high rate of positive change, and that the magnitude of the conversion process by the meridional gradient of the basic zonal flow was comparable to that of the increasing rate of local eddy kinetic energy, indicating that interaction between the eddy and the meridional gradient of the basic zonal flow was important in barotropic energy generation.

On 26 April (Figs. 3d and 3e), although the maximum centers of the increasing rate in local eddy energy and the dominant conversion term did not match exactly, the areas with large values of the latter roughly corresponded to those of the former over the BOB. Moreover, the magnitudes of these terms, especially for the southern maximum center of barotropic energy conversion (Fig. 3d), showed a slight increase rather than the decrease recorded on the previous day (Fig. 3b). Although an increase of eddy kinetic energy through the barotropic process implies that both easterly and westerly jets should decrease since zonal kinetic energy of the jets is converted into eddy kinetic energy, the strength of jets may not always weaken. As was shown in Figs. 2c and 2d, the westerly velocity between 2.5°N and 7.5°N (especially at 850 hPa) exhibited an increase rather than a decrease with time during the period 24–27 April. Such a strengthened westerly jet within 2.5°–7.5°N could be attributed to the intensification and maintenance of a cross-equatorial pressure gradient under geostrophic approximation. As noted in previous studies (e.g. Lindzen and Nigam, 1987; Tomas et al., 1999), SST is one of thermal influences on surface pressure gradients. Note that in 2008, SST in the NIO had reached 29°C–30°C till 17 April, as was mentioned in the introduction section. In fact, such high SST still sustained in the Bay of Bengal during the second half of April (McPhaden et al., 2009), forming a large-scale meridional SST gradient with cold SST to the south of the equator, and thereby creating a cross-equatorial surface pressure gradient (Lindzen and Nigam, 1987). Such cross-equatorial pressure gradient due to SST difference can maintain a zonal component of the geostrophic flow around the equator, and the intensity of the basic zonal flow is basically determined by the cross-equatorial pressure gradient (Tomas et al., 1999). Therefore, the equatorial westerly jet could be strengthened due to the enhanced cross-equatorial pressure gradient, although some of its kinetic energy was converted into the eddy kinetic energy. In addition, as compared with 24 April,

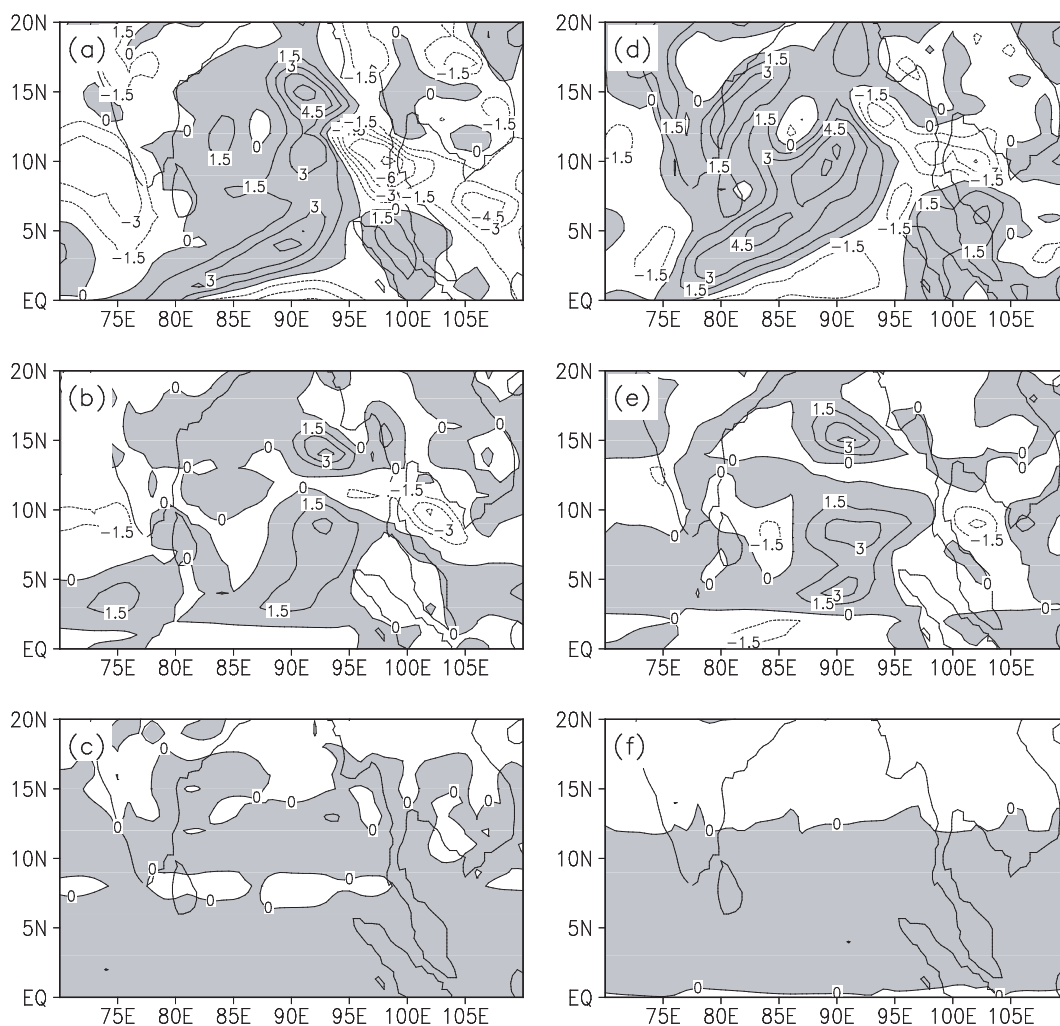


Fig. 3. (a) Local change rate of daily mean eddy kinetic energy at 850 hPa, and related barotropic energy conversion terms of (b) $-u'v'\partial[u]/\partial y$ and (c) $-v'^2\partial[v]/\partial y$ for 25 April 2008. (d)–(f) As in (a)–(c) except for 26 April 2008. Contour interval is $1.5 \times 10^{-4} \text{ m}^2 \text{ s}^{-3}$. Positive values are shaded.

a strong westerly jet after that day was noted to migrate northward significantly (Fig. 1), which could also be helpful to understand the strengthened westerly jet. These questions will be further investigated in the future, as the primary purpose of the present study is to address the effect of large-scale environmental flow on the initial growth of Nargis.

The above observations suggest that during the early developing stage of Nargis, it obtained requisite kinetic energy from the unstable basic zonal flow that was composed of the tropical–subtropical easterly jet and the equatorial westerly jet via barotropic eddy–mean flow interaction, and whereby the easterly jet tended to weaken. Whereas, the westerly jet sustained and even enhanced within 2.5° – 7.5° N due to the cross-equatorial pressure gradient as it transferred its kinetic energy to the eddy. In turn, this enhanced westerly jet could result in maximum barotropic en-

ergy conversion over the southeastern BOB (Fig. 3d) due to the increased meridional gradient of the westerly jet. Also of note is the fact that the second term on the rhs of Eq. (2) contributed little to the growth of Nargis (Fig. 3f). The magnitude of the third and fourth terms (not shown) was even less than that of the second term, suggesting that baroclinic energy conversions made a smaller contribution than did barotropic energy conversions during this developing stage.

In fact, barotropic energy conversions at 700 hPa (not shown) showed more robust and definitive signals than those at 850 hPa. During each of these two days (25–26 April), the increase in local eddy energy was concentrated over the central BOB, where the magnitude exceeded $3 \times 10^{-4} \text{ m}^2 \text{ s}^{-3}$, matching the distribution of the dominant conversion term. This finding indicates that barotropic energy conversion by horizontal shear of the basic zonal flow was indeed an im-

portant energy source for Nargis.

4. Summary and discussion

NCEP FNL analysis data were used to examine the dynamical mechanism of the formation and intensification of tropical cyclone Nargis during its formative stage, focusing on the positive role of barotropic instability of lower-tropospheric basic zonal flow, especially the contribution of the strong tropical–subtropical easterly jet within this zonal flow.

The daily evolution of low-level winds during the period 22–24 April 2008 shows that the initiation of Nargis was associated with strong equatorial westerlies. These westerlies, combined with strong tropical–subtropical easterlies, made up of a large-scale parallel shear flow, created cyclonic vorticity over the southern BOB and thereby facilitated the incipient disturbance to evolve into Nargis. The meridional distribution of absolute vorticity demonstrates that this basic shear flow was barotropically unstable, with a positive correlation between the mean zonal flow and the meridional gradient of absolute vorticity, favoring an increase in eddy energy via barotropic eddy–mean flow interactions. The maximum wind speeds of the easterly and westerly jets in the lower troposphere decreased significantly day-by-day from 24 to 27 April, with the amplified disturbance gaining more kinetic energy from the easterly jet than from the westerly jet during 25–26 April, indicating that the low-level easterly jet may have played a more important role than the westerly jet in the rapid growth of Nargis. Furthermore, the occurrence of an unstable easterly jet may be an important factor in monitoring and predicting TC activity. Additional similar case studies are necessary to confirm the effect of the easterly jet on TC formation.

Energetics analysis for the period 25–26 April showed that the barotropic conversion term by the interaction between the eddy and the meridional gradient of the basic zonal flow was dominant, with its magnitude comparable to the local increasing rate of eddy kinetic energy; other terms made only minor contributions to the growth of Nargis. Thus, barotropic energy conversion by horizontal shear of the basic zonal flow was indeed an important energy source for Nargis.

It should be noted that a barotropic mechanism cannot explain the local change rate of daily eddy kinetic energy, especially in the northwestern quadrant (Figs. 3d and 3e), which implies that a diabatic process may play a role in intensification when a TC attains a finite strength. Because the incipient disturbance that evolved into Nargis was initiated by the MJO, its development was inevitably related to diabatic processes because the MJO convection releases

a large amount of latent heat. Accordingly, in the future, we intend to investigate related issues in terms of the contribution of baroclinic energy conversion to eddy intensification during the developing and mature stages of Nargis. We did not examine the role of baroclinic dynamics in the present case study because we focused on the formation stage of Nargis, during which barotropic instability played a more important role than during the mature stage, as discussed above. Although Nargis may be a representative case in which barotropic instability made a greater contribution to rapid TC growth during the formation stage, further research is required to determine whether the relationship holds true in other cases.

Acknowledgements. The NCEP FNL data analyzed in this study were obtained from the Research Data Archive (RDA) at the National Center for Atmospheric Research (NCAR). This research was jointly supported by the Knowledge Innovation Program of the Chinese Academy of Sciences (KZCX2-YW-Q11-04), the National Basic Research Program of China (2010CB950401), and the National Natural Science Foundation of China (Grant Nos. 40975052, 40875034, and 40821092).

REFERENCES

- Chen, G., and R. Huang, 2008: Influence of monsoon over the warm pool on interannual variation on tropical cyclone activity over the western North Pacific. *Adv. Atmos. Sci.*, **25**, 319–328, doi: 10.1007/s00376-008-0319-7.
- Eliassen, A., 1983: The Charney–Stern theorem on barotropic–baroclinic instability. *Pure Appl. Geophys.*, **121**, 261–285.
- Ferreira, R. N., and W. H. Schubert, 1996: Dynamical aspects of twin tropical cyclones associated with the Madden–Julian oscillation. *J. Atmos. Sci.*, **53**, 929–945.
- Ferreira, R. N., and W. H. Schubert, 1997: Barotropic aspects of ITCZ breakdown. *J. Atmos. Sci.*, **54**, 261–285.
- George, L., and S. K. Mishra, 1993: An observational study on the energetics of the onset monsoon vortex, 1979. *Quart. J. Roy. Meteor. Soc.*, **119**, 755–778.
- Gill, A. E., 1980: Some simple solutions for heat-induced tropical circulation. *Quart. J. Roy. Meteor. Soc.*, **106**, 447–462.
- Gray, W. M., 1968: Global view of the origin of tropical disturbances and storms. *Mon. Wea. Rev.*, **96**, 669–700.
- Gray, W. M., 1975: Tropical cyclone genesis. Department of Atmospheric Science Paper No. 234, Colorado State University, Fort Collins, CO, 121pp.
- Guinn, T. A., and W. H. Schubert, 1993: Hurricane spiral bands. *J. Atmos. Sci.*, **50**, 3380–3403.
- Harr, P. A., and R. L. Elsberry, 1995: Large-scale cir-

- ulation variability over the tropical western North Pacific Part I: Spatial patterns and tropical cyclone characteristics. *Mon. Wea. Rev.*, **123**, 1225–1246.
- Holland, G. J., 1993: The Global Guide to Tropical Cyclone Forecasting. WMO/TD-560, World Meteorological Organization, Geneva, 342pp.
- Kikuchi, K., B. Wang, and H. Fudeyasu, 2009: Genesis of tropical cyclone Nargis revealed by multiple satellite observations. *Geophys. Res. Lett.*, **36**, L06811, doi: 10.1029/2009GL037296.
- Krishnamurti, T. N., P. Ardanuy, and Y. Ramanathan, R. Pasch, 1981: On the onset vortex of the summer monsoons. *Mon. Wea. Rev.*, **109**, 344–363.
- Kuo, H. L., 1949: Dynamical instability of two-dimensional non-divergent flow in a barotropic atmosphere. *J. Meteor.*, **6**, 105–122.
- Liebmann, B., H. H. Hendon, and J. D. Glick, 1994: The relationship between tropical cyclones of the western Pacific and Indian Oceans and the Madden–Julian oscillation. *J. Meteor. Soc. Japan*, **72**, 401–411.
- Lindzen, R. S., and S. Nigam, 1987: On the role of the sea surface temperature gradients in forcing low level winds and convergence in the tropics. *J. Atmos. Sci.*, **44**, 2418–2436.
- Lorenz, E. N., 1955: Available potential energy and the maintenance of the general circulation. *Tellus*, **7**, 157–167.
- Madden, R. A., and P. R. Julian, 1994: Observations of the 40–50 day tropical oscillation—A review. *Mon. Wea. Rev.*, **122**, 814–837.
- Maloney, E. D., and D. L. Hartmann, 2001: The Madden–Julian oscillation, barotropic dynamics, and North Pacific tropical cyclone formation, Part I: Observations. *J. Atmos. Sci.*, **58**, 2545–2558.
- Mao, J., and G. Wu, 2010: Intraseasonal modulation of tropical cyclogenesis in the western North Pacific: A case study. *Theor. Appl. Climatol.*, **100**, 397–411.
- McPhaden, M. J., and Coauthors, 2009: Ocean–atmosphere interactions during cyclone Nargis. *EOS, Transactions, American Geophysical Union*, **90**, 53–60.
- Mishra, S. K., M. D. Patwardhan, and L. George, 1985: A primitive equation barotropic instability study of the monsoon onset vortex, 1979. *Quart. J. Roy. Meteor. Soc.*, **111**, 427–444.
- Nitta, T., and K. Masuda, 1981: Observational study of a monsoon depression developed over the Bay of Bengal during summer MONEX. *J. Meteor. Soc. Japan*, **59**, 672–682.
- Nitta, T., and M. Yanai, 1969: A note on the barotropic instability of the tropical easterly current. *J. Meteor. Soc. Japan*, **47**, 127–130.
- Norquist, D. C., E. E. Recker, and R. J. Reed, 1977: The energetics of African wave disturbances as observed during phase III of GATE. *Mon. Wea. Rev.*, **105**, 334–343.
- Ross, R. S., 1991: Energetics of African wave disturbances derived from the FSU global spectral model. *Meteor. Atmos. Phys.*, **45**, 139–158.
- Ross, R. S., and T. N. Krishnamurti, 2008: barotropic energy conversion as a predictor of development for NAMMA African easterly waves. *Proc. 28th Conf. on Hurricanes and Tropical Meteorology*, Orlando, FL, Amer. Meteor. Soc., 7–10.
- Shenoi, S. S. C., D. Shankar, and S. R. Shetye, 1999: On the sea surface temperature high in the Lakshadweep Sea before the onset of the southwest monsoon. *J. Geophys. Res.*, **104**, 15703–15712.
- Subrahmanyam, D., M. K. Tandon, L. George, and S. K. Mishra, 1981: Role of barotropic mechanism in the development of a monsoon depression: A MONEX study. *Pure Appl. Geophys.*, **119**, 901–912.
- Tomas, R., R. Holton, and P. J. Webster, 1999: The influence of cross-equatorial pressure gradients on the location of near-equator convection. *Quar. J. Roy. Meteor. Soc.*, **125**, 1107–127.
- Wheeler, M. C., and H. H. Hendon, 2004: An all-season real-time multivariate MJO index: Development of an index for monitoring and prediction, *Mon. Wea. Rev.*, **132**, 1917–1932.
- Zehr, R. M., 1992: Tropical cyclogenesis in the western North Pacific. NOAA Tech. Rep. NESDIS 61, Department of Commerce, Washington DC.
- Zhou, W., and J. C. L. Chan, 2005: Intraseasonal oscillations and the South China Sea summer monsoon onset. *Int. J. Climatol.*, **25**, 1585–1609.